QUARTERLY OF APPLIED MATHEMATICS

Vol. XXX JULY 1972 No. 2

"ESCAPE" FROM A POTENTIAL WELL (PART II)*

BY

R. SUBRAMANIAN AND R. E. KRONAUER

Harvard University

1.0 Introduction. We will now consider the "escape" problem described in Part I [1] modified by the addition of linear dissipative forces. All solutions now can be expected to be of basically two types:

(1) Motions that constitute solutions decaying asymptotically down to the origin ($x_1 = 0, x_2 = 0$).

(2) Solutions that "escape" with or without an initial decay process that is characterized by amplitude reduction in the coordinates x_1 , x_2 .

In Part I the conservative trapped motions were related to the stability transitions along the loci of the families of periodic motions. In the presence of dissipation the amplitudes of the periodic motions are progressively decreasing and the "escape" problem will be related to the nature of the decaying periodic motion.

The contents of this study will be described in two sections. Sec. 2.0 discusses dissipation effects in a simplified problem, the results of which will then prove helpful in understanding the complete problem described in Sec. 3.0.

2.0. Simplified problem (in the absence of the "lip"). The phenomena associated with the addition of dissipative forces can be understood more easily by considering first the simpler problem where the cubic term in x_2 is absent from the potential energy function $V(x_1 , x_2)$ (For a definition of $V(x_1 , x_2)$, see (2.1) of Part I.) Thus, in the absence of the "lip" the equations of motion with added linear dissipative forces are

$$\frac{d^2x_1}{dt^2} + \epsilon\mu \frac{dx_1}{dt} + x_1(1 - \epsilon\nu) = 2\epsilon x_1 x_2 , \tag{2.1}$$

$$\frac{d^2x_2}{dt^2} + \epsilon\eta \frac{dx_2}{dt} + 4x_2 = \epsilon x_1^2 . \tag{2.2}$$

Here μ, η are assumed positive and the small parameter ϵ is taken as equal to 0.1.

For the weakly coupled conservative system ($\eta = \mu = 0$) Kronauer and Musa [2] have shown the existence of two adiabatic invariants of motion. These invariants are found by truncating the series solution for the modal amplitudes and phases at some order of the expansion parameter. The invariants obtained at the first approximation are

* Received March 12, 1971. This work and *"Escape" from a potential well (part I)* were supported in part by the Navy under contract N00014-67-A-0298-0006, and by the Division of Engineering and Applied Physics, Harvard University.

$$R_{01}^2 + 4R_{02}^2 = \text{constant} \equiv \bar{E}_0^2 , \tag{2.3}$$

$$R_{01}^2 R_{02} \cos(2\phi_{01} - \phi_{02}) - 4\nu R_{02}^2 = \text{constant}. \tag{2.4}$$

Utilizing Gilchrist's transformation [3] to χ, ψ_0 coordinates defined by

$$\sin\chi = \frac{2R_{02}}{\bar{E}_0}; \qquad \cos\chi = \frac{R_{01}}{\bar{E}_0} \quad \text{and} \quad \psi_0 = 2\phi_{01} - \phi_{02},$$

we have from (2.4)

$$\sin\chi \cos^2\chi \cos\psi_0 - \frac{2\nu}{\bar{E}_0}\sin^2\chi = \text{constant} \equiv K. \tag{2.5}$$

Fig. 1 shows some typical integral curves in the $\chi - \psi_0$ plane given by (2.5), for cases with and without detuning. It may be noted that as the detuning parameter ν increases, the singular points P and Q move towards the limits $\chi = 0$ and $\chi = \pi/2$ respectively. At the same time the saddles S and V move toward each other. Identical behavior is observed if $\bar{E}_0$ is decreased while maintaining ν at some constant nonzero value.

In the presence of dissipation $\bar{E}_0^2$ and K are in general no longer constant. If $x_1(t)$ and $x_2(t)$ are assumed to be of the form

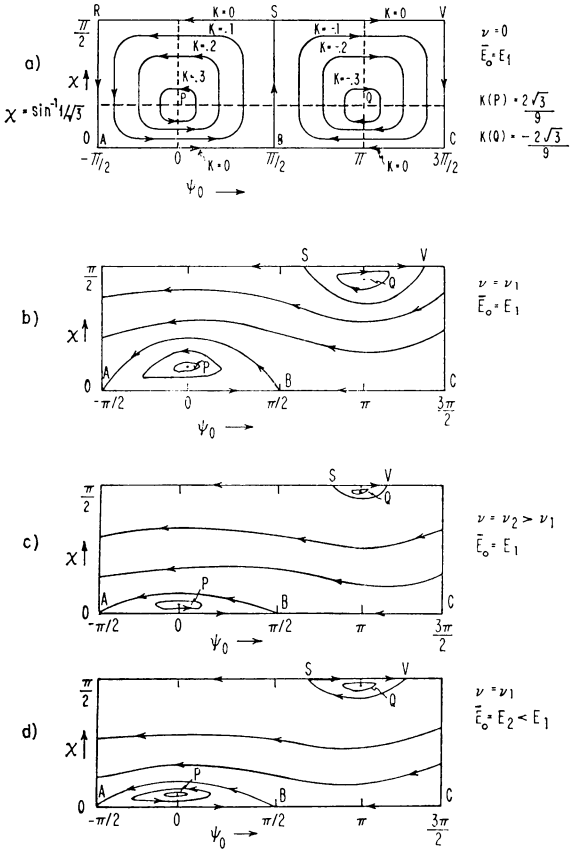

FIG. 1. Integral curves on $\chi - \psi_0$ plane.

$$x_1(t) = R_{01} \cos(t + \phi_{01}) + O(\epsilon) \text{ terms}, \tag{2.6}$$

$$x_2(t) = R_{02} \cos(2t + \phi_{02}) + O(\epsilon) \text{ terms}, \tag{2.7}$$

where R_{01}, R_{02}, ϕ_{01}, ϕ_{02} are slowly varying functions of time, then a first-order analysis with inclusion of dissipation yields:

$$dR_{01}/dt = (-\epsilon/2)[R_{01}R_{02} \sin(2\phi_{01} - \phi_{02}) + \mu R_{01}], \tag{2.8}$$

$$dR_{02}/dt = (\epsilon/8)[R_{01}^2 \sin(2\phi_{01} - \phi_{02}) - 4\eta R_{02}], \tag{2.9}$$

$$R_{01}(d\phi_{01}/dt) = (-\epsilon/2)[R_{01}R_{02} \cos(2\phi_{01} - \phi_{02}) + \nu R_{01}], \tag{2.10}$$

$$R_{02}(d\phi_{02}/dt) = (-\epsilon/8)R_{01}^2 \cos(2\phi_{01} - \phi_{02}). \tag{2.11}$$

Assuming zero detuning for simplicity, the differential equations satisfied by $\bar{E}_0^2$ and K are now found to be

$$d\bar{E}_0^2/dt = -\epsilon\bar{E}_0^2(\eta \sin^2 \chi + \mu \cos^2 \chi), \tag{2.12}$$

$$dK/dt = (-\epsilon K/2)(\eta - \mu)(1 - 3 \sin^2 \chi). \tag{2.13}$$

The expressions (2.12) and (2.13) indicate that the average energy decay is proportional to $(\eta + \mu)$ whereas the variation of K is dependent on $(\eta - \mu)$. The integral curves representation is now more complicated and the trajectories would have to be portrayed in three-dimensional space with χ, ψ_0 and $\bar{E}_0$ as coordinates. However, we can still consider $\chi - \psi_0$ planes of successively decreasing energies and analyse the nature of the trajectories. The differential equation for the $\chi - \psi_0$ phase plane becomes

$$\frac{d\chi}{d\psi_0} = \frac{[\bar{E}_0 \sin \psi_0 \cos \chi - \Omega \sin 2\chi] \sin \chi}{[\bar{E}_0 \cos \psi_0(1 - 3 \sin^2 \chi) - 4\nu \sin \chi]} \tag{2.14}$$

where $\Omega = \eta - \mu$.

Fig. 2 shows the trajectories in the $\chi - \psi_0$ plane for different values of the parameter $q = (\eta - \mu)/2\bar{E}_0$ corresponding to a progressive decay of $\bar{E}_0$. The arrows marked denote the instantaneous direction of motion within a $\chi - \psi_0$ plane. Of course as time advances we must also advance from plane to plane in a sequence of decreasing energy. We can follow the character of the solutions approximately by considering successive $\chi - \psi_0$ planes.

In the sequence of diagrams in Fig. 2, two different decay processes can be seen. Within each diagram the motions are converging towards stable singular points such as P or Q in Fig. 2(a) or T in Fig. 2(e). This is the decay process characterized by (2.13). In addition to this there is the general decay of energy which carries the system from diagram to diagram and causes the singular points to move and coalesce. Fig. 2(d) shows the coalescence of two foci and one saddle. Now in the full three-dimensional phase space $(\chi, \psi_0, \bar{E}_0)$ there are no true singular points except at $\bar{E}_0 = 0$; however, these points of zero velocity for components measured in the $\chi - \psi_0$ plane do characterize regions of the three-dimensional field toward which trajectories converge. Note that the final asymptotic state of the system is $\chi \to 0$. This means that asymptotically the residual energy of the system is in the x_1 oscillation, a fact consistent with the larger dissipation in the x_2 oscillator.

Fig. 3 shows the situation for $\mu > \eta$. It is equally interesting that at the high energy-level (Fig. 3(a)) there is no stable singularity in the two-dimensional field. This means

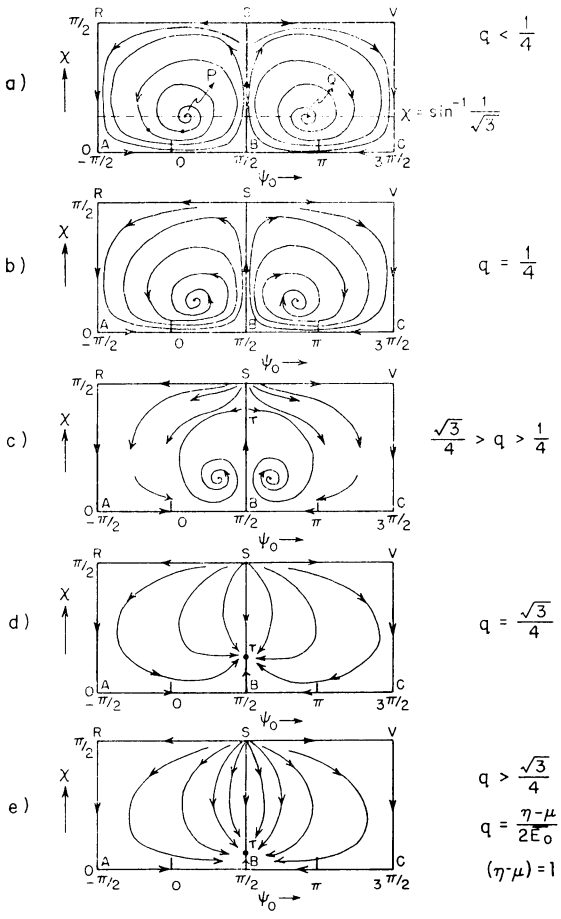

FIG. 2. Integral curves on $\chi - \psi_0$ plane in presence of damping and zero detuning [$\eta > \mu$].

that during the early stages of energy decay from a high level the energy will tend to exchange back and forth between the two oscillators. At lower energy levels (Fig. 3(c)) stable singularities arise at R and V and these persist down to $\bar{E}_0 = 0$. Once again we see that the residual energy ends up in the oscillator with the lesser dissipation (x_2 here). It is interesting to note that in both Figs. 2 and 3 the stable singularity at very low energy is a node. This is consistent with the fact that the energy exchange process, being nonlinear in origin, becomes progressively less important as the energy decreases and in the limit the decay of the two oscillators proceeds quite independently.

An interesting case is obtained when there are equal damping constants in both coordinates ($\eta = \mu$). The integral curves are then *identical* to those for conservative oscillations and the total energy decays exponentially as

$$\bar{E}_0^2(t) = \bar{E}_0^2(0) \exp(-\epsilon\eta t). \tag{2.15}$$

The energy exchange process is no different from that for conservative oscillations but occurs progressively more slowly at progressively decreasing amplitudes of x_1 and x_2.

The addition of detuning modifies the integral curves considerably; Fig. 4 shows some

typical examples. A decrease of the system energy causes a drift of the stable foci P, P' toward the *stationary* saddles B and J respectively. In contrast, the unstable foci Q and Q' drift toward the *nonstationary* equilibrium points S and E. There is a critical value of the (q, p) pair when S and E coalesce with Q and Q' respectively, following which S and E transform into unstable nodes. Furthermore, R and V drift along χ equal to $\pi/2$ toward E and S. Their subsequent coalescence occurs at an energy lower than that necessary for the formation of nodes at E and S.

As the energy continues to decay the trajectories are eventually directed towards the stable foci P, P' which in turn approach the asymptote χ equal to zero. However, the number of cycles of ψ_0 executed before termination at the stable foci increases in proportion to the initial value of χ. In contrast to the case for zero detuning, the trajectories are all parallel to the ψ_0 axis at very low energy levels, indicative of the fact that the detuning which causes the steady change of phase is linear and hence dominates over the nonlinear energy exchange process.

A reversal of the sign of $\Omega = (\eta - \mu)$ causes the trajectories to be directed eventually toward χ equal to $\pi/2$, as seen in Fig. 5.

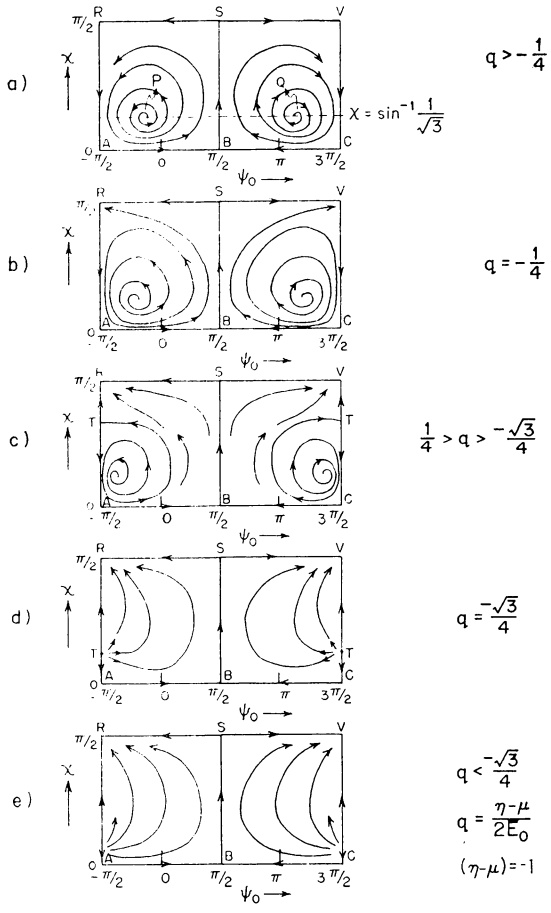

FIG. 3. Integral curves on $\chi - \psi_0$ plane in presence of damping and zero detuning [$\eta < \mu$].

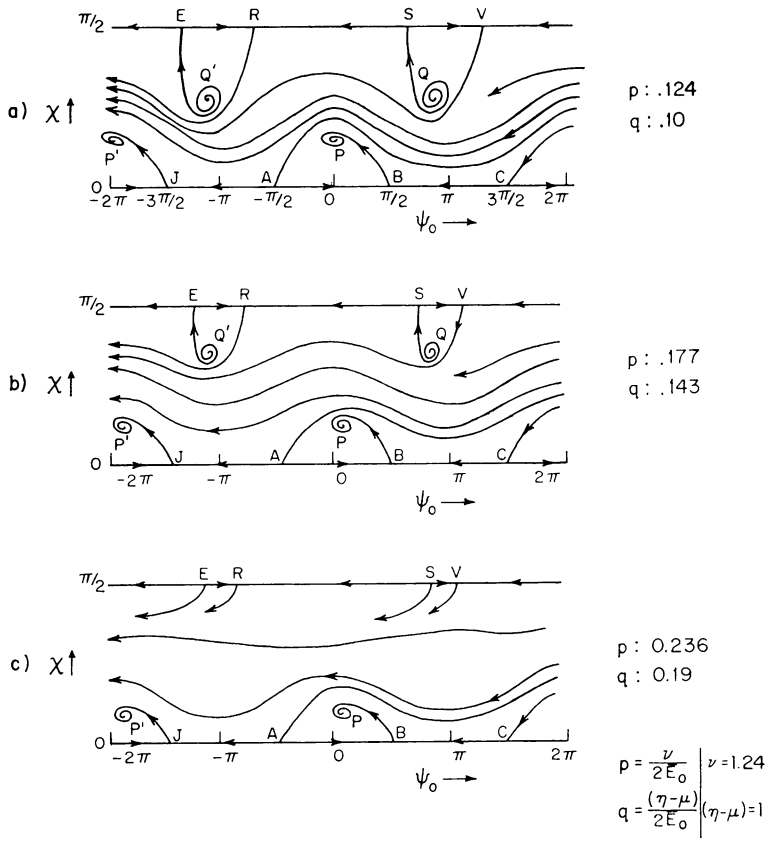

FIG. 4. Integral curves in $\chi - \psi_0$ plane in the presence of damping and detuning [$\eta > \mu$].

For equal damping constants ($\eta = \mu$) the integral curves for fixed ν are similar to those shown in Fig. 1(b) and (d). If the initial conditions $\chi(0)$, $\psi_0(0)$ coincide with either of the equilibrium points P or Q the system decays towards the asymptotic values of χ, maintaining a constant phase of 0 or π. The asymptotic behavior for very low energies consists of trajectories parallel to the ψ_0 axis.

3.0. Complete problem (including the "lip"). Having described the kinds of motions that occur for the simpler problem, we shall now consider the complete problem in the presence of the "lip".

The differential equations of motion in the presence of dissipation and with the "lip" included are

$$\frac{d^2x_1}{dt^2} + \epsilon\mu \frac{dx_1}{dt} + x_1(1 - \epsilon\nu) = 2\epsilon x_1 x_2 , \tag{3.1}$$

$$\frac{d^2x_2}{dt^2} + \epsilon\eta \frac{dx_2}{dt} + 4x_2 + 3x_2^2 = \epsilon x_1^2 . \tag{3.2}$$

An examination of Fig. 6 (reproduction of Fig. 6 in Part I) suggests that the study with dissipation might be most interesting for values of ν in the range $2 > \nu > 0$. In

particular one could ask: "What is the character of decay for a solution which in the absence of dissipation would be trapped at a high energy level corresponding to a Family 2 solution?" Since Fig. 6 shows the existence of divergent solutions at energies through which the system must pass if it is to decay asymptotically to the origin, it might be expected that escape from the potential well would be a necessary consequence of dissipation. As we shall see, this is not always the case. There are two ways in which stable decay to the origin can occur. One is with *very large* dissipation which removes most of the energy from the system in very few oscillations. The other is with properly arranged small dissipation that drives the system toward a decaying Family 2 type periodic solution. Fig. 7 (Fig. 12 of Part I) shows that for $\nu \geq 1.3$ there are branches of this family that extend from near the origin to high energy levels. Figs. 8a, 8b, and 8c show approximate sketches of the trapped regimes for the indicated values of ν. There is a sharp narrowing at Q for $\nu = 1.3$ and a subsequent break-up of this region for lower values of ν.

Let us consider now the initial conditions $x_2(0) = x_1(0) = (dx_2/dt)(0) = 0$ and $(dx_1/dt)(0) \neq 0$ which were used to generate Fig. 6. If we assume that the analysis of Sec. 2.0 can be applied in some approximate sense here, then we expect that for $\eta > \mu$ solutions will decay toward the synchronized periodic motions. Then, if the initial condition $(dx_1/dt)(0)$ is not too far removed from the locus of periodic solutions, we would

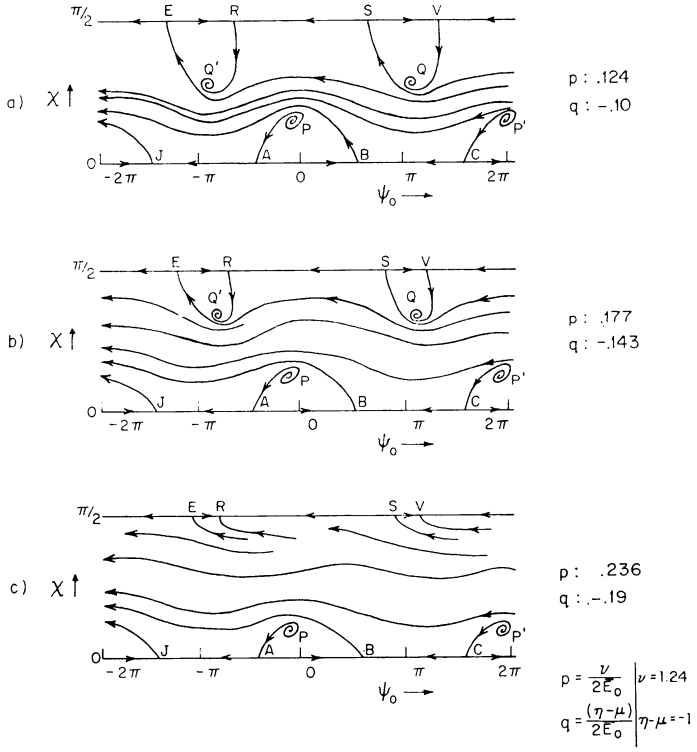

FIG. 5 Integral curves in $\chi - \psi_0$ plane in the presence of damping and detuning [$\eta < \mu$].

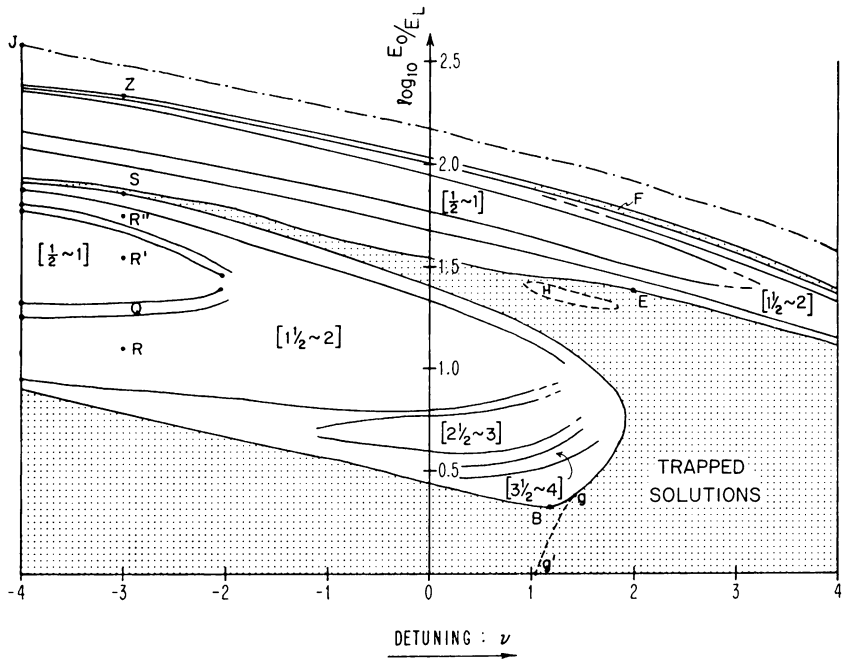

FIG. 6. Plot of logarithm of normalized escape energy versus detuning ν $[-4 \leq \nu \leq +4]$.

expect this decay to take place quite rapidly and the system could then decay to lower energies along or near the locus. If the locus proceeds continuously toward zero energy as it does for $\nu \geq 1.3$ the trajectory can be expected to remain trapped throughout the decay process.

Even if there is a break in the locus of periodic solutions, as at Q' in Fig. 8(c), a modest amount of dissipation can permit the system to "jump the gap" and continue to decay without escape.

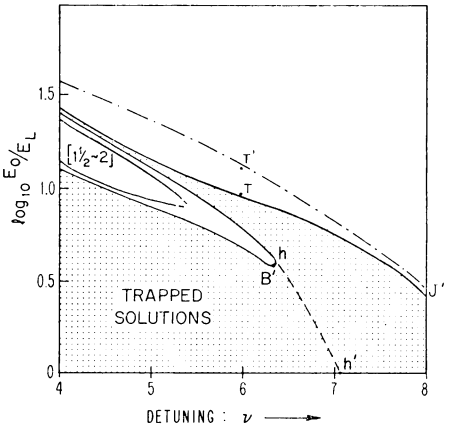

FIG. 6a. Plot of logarithm of normalized escape energy versus detuning ν $[4 < \nu < 8]$.

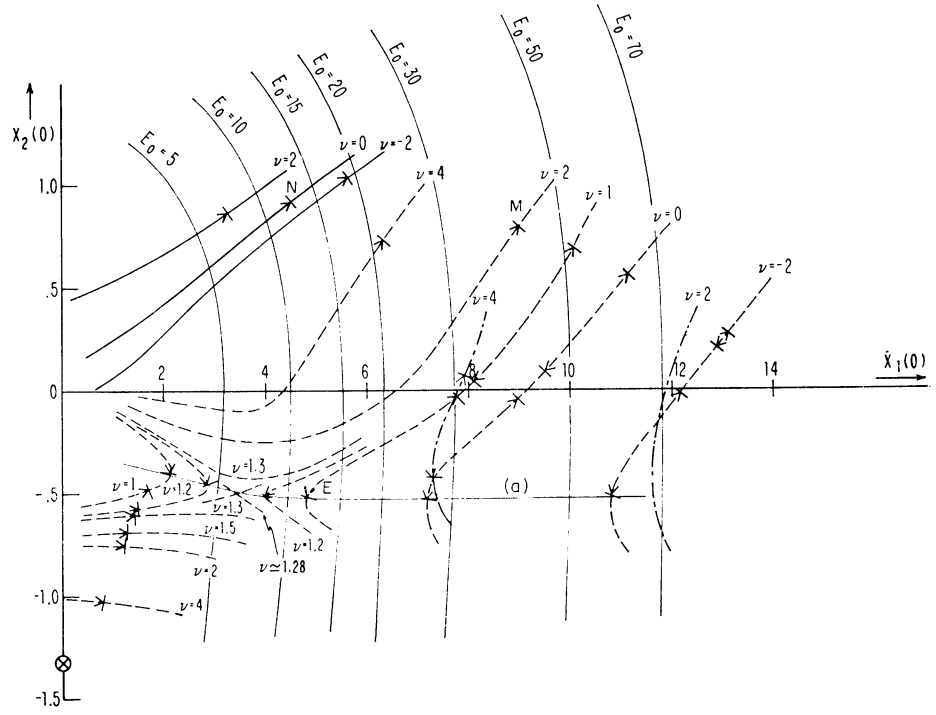

FIG. 7. Plot of family of periodic solutions for different values of deturning ν. Legend: $\otimes$: Position of "lip"; ——— : Family #1; - - - - : Family #2; — - — - —: Family #3; →|: Limit of trapped solution; (a): Locus of vertical tangents to Family 2 solutions.

The problem at hand has two parameters, the initial energy (equivalent to $(dx_1/dt)(0)$) and the detuning ν. For any set of these we can determine values of η and μ which lead to escape or stable asymptotic decay. The results are shown in Figs. 9a, 9b, 9c. The figures show the demarcation lines (for different ν) in the $\eta - \mu$ space that separate the stably decaying solutions from those that "escape." These results were obtained from simulation studies on the analogue computer and each of the figures refers to a particular initial energy level.

Considering Fig. 9a, we see that for $\eta > \mu$ the dissipation necessary for asymptotic decay decreases with an increase in ν, in agreement with our earlier hypothesis. From Fig. 9b we observe again that for $\nu \lesssim 1.3$ progressively increasing dissipation is necessary

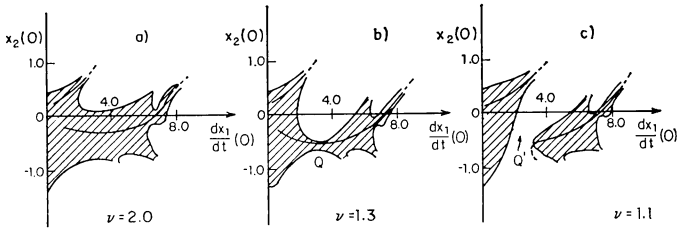

FIG. 8. Regions of trapped solutions for $1.0 < \nu \leq 2.0$.

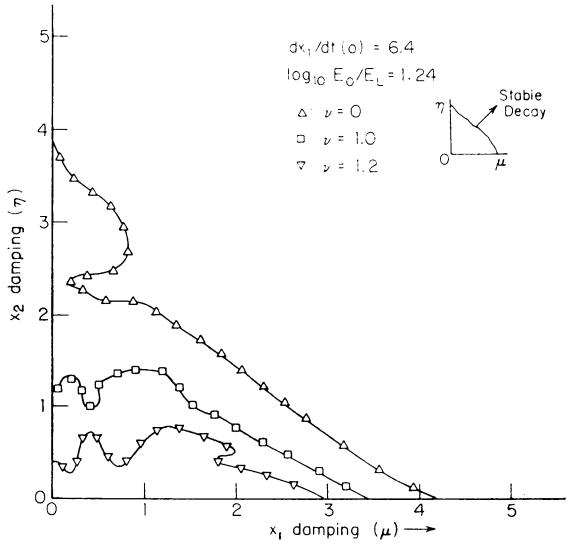

FIG. 9(a). Demarcation boundaries between "escape" and trapped solutions in the presence of damping forces.

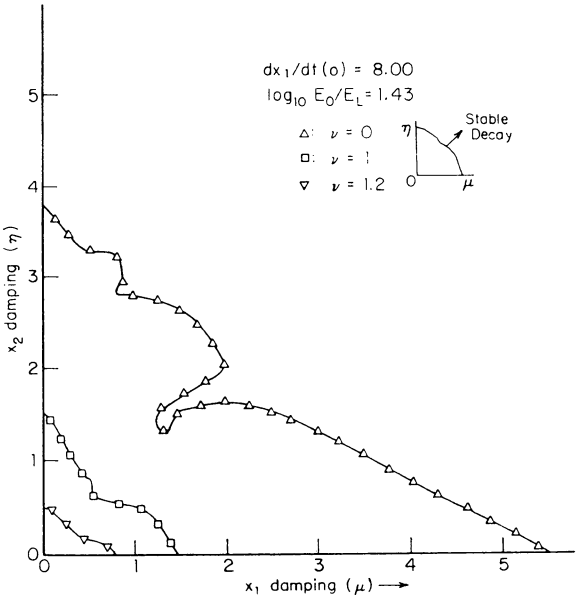

FIG. 9(b). Demarcation boundaries between "escape" and trapped solutions in the presence of damping forces.

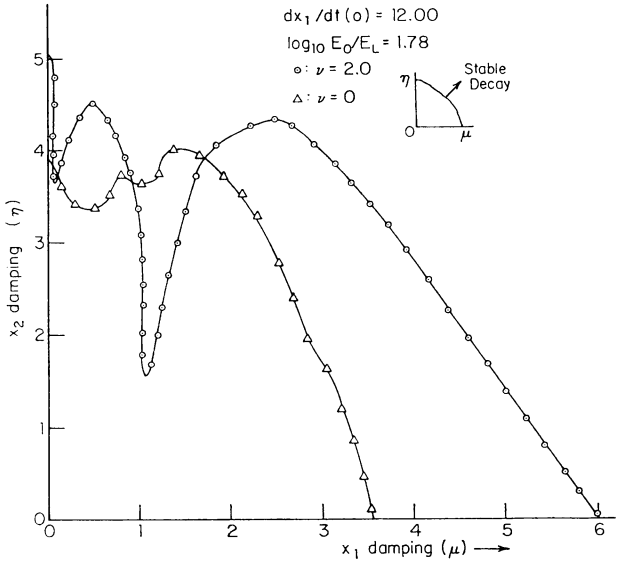

FIG. 9(c). Demarcation boundaries between "escape" and trapped solutions in the presence of damping forces.

for stabilization. Fig. 9c corresponds to a very high-energy initial condition and shows that even for $\nu = 2.0$ we require now relatively much heavier dissipation than in the earlier two cases. Note the sharp "dip" in the locus for $\nu = 2$ (Fig. 9c), the significance of which will be considered below.

Fig. 10a shows an example of a decaying solution in $x_1 - x_2$ space. The solution becomes unbounded after three or four cycles of oscillation. Remarkably, an increased

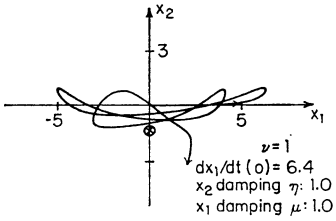

FIG. 10(a). "Escape" solution.

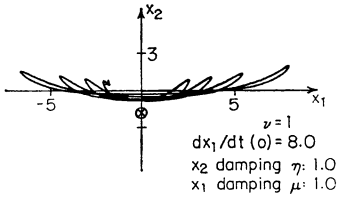

FIG. 10(b). Asymptotic decay.

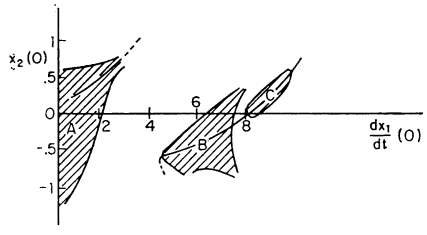

FIG. 11. Trapped regimes for $\nu = 1.0$ [Fig. 27 of Part I].

value of the initial energy causes the solution to decay asymptotically to the origin (Fig. 10b). From Fig. 11 we notice that when $(dx_1/dt)(0)$ is 6.4 the motion is quite far removed from a Family 2 periodic solution and is in an adverse location for negotiating the "jump" from region B to region A necessary for stable decay. In contrast, an initial condition of $dx_1/dt = 8.0$ is very close to the locus of periodic solutions and the decay proceeds in that direction. Note that the decay process has to make a transition first from region C to region B and then another one from B to A. Both of these are accomplished with a dissipation that decreases the amplitude of the pseudo-periodic motion by about one-third in each complete cycle. The solution shown in Fig. 10a is characterized by a sizable transfer of energy to the x_2 coordinate during the decay process and subsequent "escape."

Figs. 12a and 12b show examples of decay from a very high initial energy level. The solution in Fig. 12a has an initial energy neighboring that for a Family 3 periodic solution. The damping constants are of the right relative magnitude to cause the solution to decay stably to the origin. A slight *increase* in μ, however, causes the solution to be divergent, as seen in Fig. 12b.

The explanation is that the decay toward the periodic solution is caused by $\eta - \mu$, so that raising μ decreases this effect. Actually the process of stable decay to the origin, as in Fig. 12a, is a complex series of events, requiring first a decay toward a Family 3 periodic solution, then a transition to a Family 2 periodic solution and finally a continuing loss of energy along the locus of Family 2 periodic solutions. In Fig. 9c it is clear from the narrow "dip" in the experimental stability boundary for $\nu = 2.0$ that only a precise balance between η and μ will permit this chain of events to occur for modest levels of damping.

3.1. Influence of dissipation on the integral curves. The mathematical analysis in Part I (Sec. 5.2) describing the amplitude and phase variations showed that the quadratic term representing the "lip" had no effect on the variations when considering first-order terms. Therefore it was necessary to consider a second-order analysis. Then the effect of the "lip" was seen, but only in the phase variations. Detuning, which affects the phase variations in the first-order analysis, has an added effect on the amplitude variations in the second-order analysis. Here we wish to include dissipation in as simple a way as possible. Thus we assume the damping constants to be sufficiently small that quadratic terms involving them can be neglected while the analysis will include second-order effects of the nonlinearities. In such a case the added terms due to dissipation occur only in the amplitude variations and are identical with those in (2.8) and (2.9).

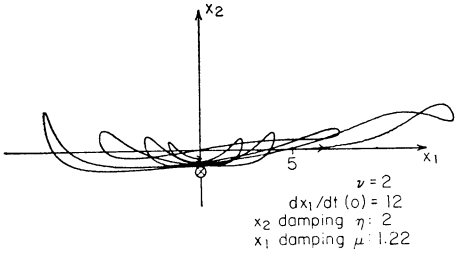

FIG. 12(a). Asymptotic decay.

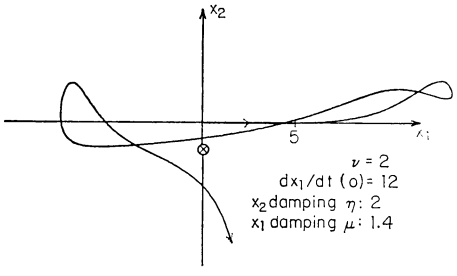

FIG. 12(b). "Escape" solution.

Otherwise the equations appear as in Sec. 5.2 of Part I. If we introduce the variables χ and ψ_0 as in that section

$$\left(\tan \chi = \frac{2R_{02}}{R_{01}(1 + .025\nu\delta)^{1/2}}\,; \qquad \psi_0 = 2\phi_{01} - \phi_{02}\right),$$

the differential equation for the $\chi - \psi_0$ phase plane with dissipation included becomes

$$\frac{d\chi}{d\psi_0} = \frac{[E_\theta \sin \psi_0 \cos \chi - \Omega \sin 2\chi] \sin \chi}{[E_\theta \cos \psi_0(1 - 3 \sin^2 \chi) + (\delta k_0/2)E_\theta^2 \sin^3 \chi + (\delta k_1 - 4\nu) \sin \chi]}. \tag{3.3}$$

Here E_θ has a slightly different distinction from $\bar{E}_0$ in order to include second-order effects due to the "lip":

$$E_\theta^2 = R_{01}^2(1 + .025\nu\delta) + 4R_{02}^2\,. \tag{3.4}$$

In (3.3) k_0 , k_1 are parameters depending on ν, E_θ and δ is the perturbation parameter (see Sec. 5.2 of Part I).

Relation (3.3) shows that for $\Omega = 0(\eta = \mu)$ the family of integral curves described in Part I can again be used to study the dissipative system. Of course since the total energy is decaying we would again have to consider $\chi - \psi_0$ planes of successively decreasing energy.

Consider a value $\nu = 2$ and equal damping constants ($\eta = \mu$). For an initial condition close to A of Fig. 13 (Fig. 30 of Part I), the solution remains trapped close to A regardless of the energy level. The ratio of x_2 amplitude to x_1 amplitude is small (since χ is small) and both amplitudes decay together as E_θ decreases. For $\nu = 1$, there is a coalescence of A with C at some low energy level and an integral curve that was closed around A at a high energy level "opens" and exhibits a monotonically increasing phase (ψ_0) at low energies. In this case a high-energy solution can still decay to the origin but only with a larger dissipation than that for $\nu = 2$. This is equivalent to jumping over the

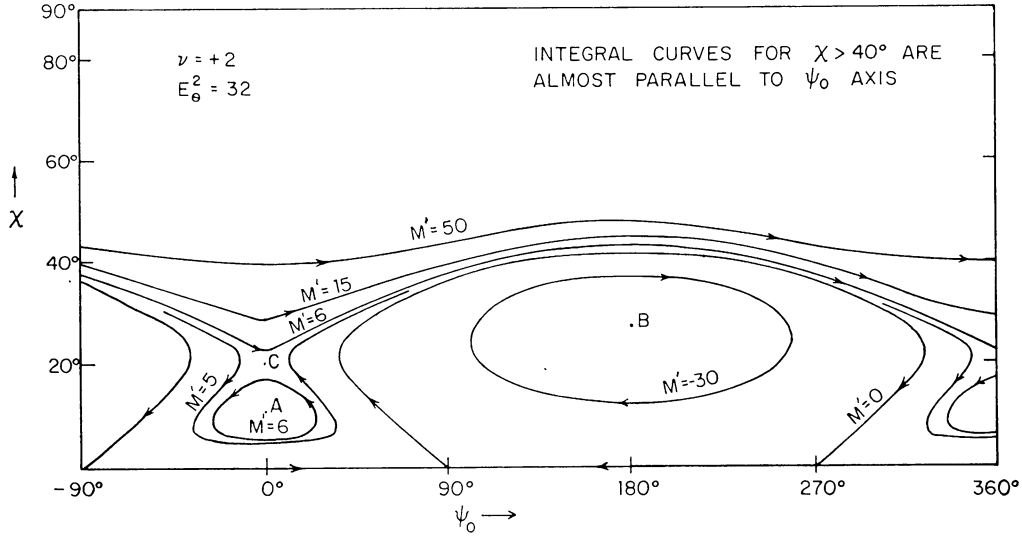

FIG. 13. Integral curves in $\chi - \psi_0$ plane.

gap Q' in Fig. 8c. For $\nu = 0$, the coalescence of the singular points A and C occurs at a still higher value of the energy, so that even *greater* dissipation would be necessary for stable decay.

For η different from μ the motion is more complicated.

Figs. 14, 15, 16 have been prepared by calculating singular points from (3.3) for selected values of $\eta - \mu$ and E_θ and then sketching the trajectories qualitatively using the linearized properties of each singular point. For $\nu = 0$ (Fig. 14), as the energy de-decreases the stable singular point B moves toward the saddle at P. For a reversed sign of $\eta - \mu$ the focus at B becomes unstable and B moves toward Q with decreasing energy.

Fig. 15 shows a typical example for $\nu \neq 0$. As the energy parameter E_θ^2 decreases, A moves toward the saddle at $\chi = 0; \psi_0 = \pi/2$ while B and C drift toward each other. The figures also show initial condition regimes that lead to an asymptotic decay, either toward A or B. Note, however, that there is no guarantee that there will be a stable decay. For the conservative case B corresponds to a Family 1 periodic motion and for $E_\theta^2 > 20$ it is unstable, a fact not evidenced from the closed integral curves surrounding B for the conservative case (the instability arising due to the generation of a one-half subharmonic). Clearly in the presence of dissipation and for high-energy initial conditions lying near B, asymptotic decay toward B as seen in Fig. 15 is not sufficient to prevent "escape." However, if the point B is stable in the absence of dissipation then for initial conditions sufficiently close to B decay toward B does ensure trapping. It has been

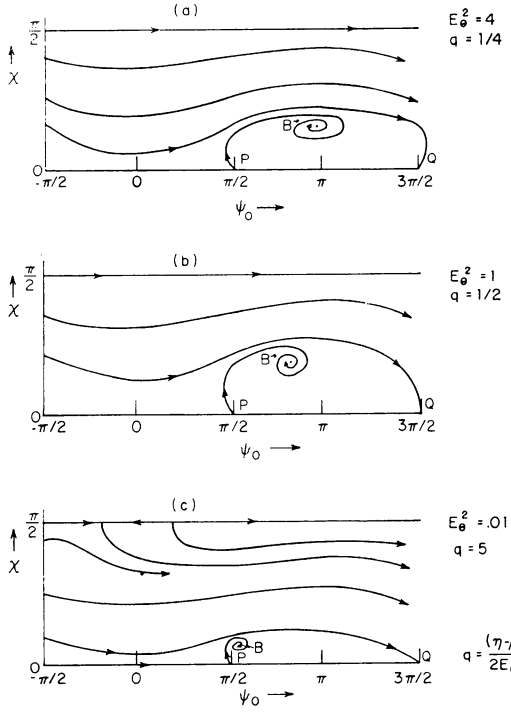

FIG. 14. Integral curves in the presence of damping ($\eta > \mu \cdot \nu = 0$).

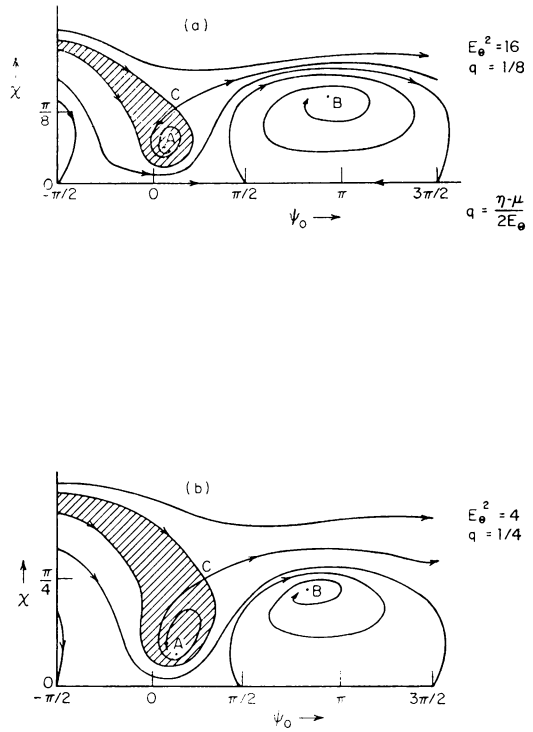

FIG. 15. **Integral curves in the presence of damping ($\eta > \mu$, $\nu = 2$).**

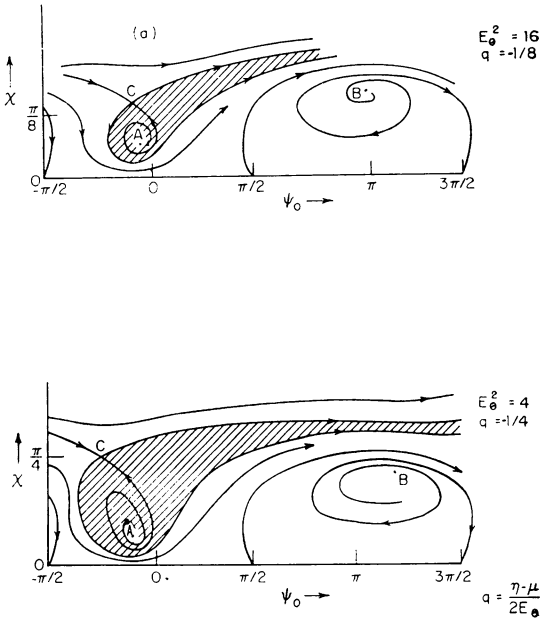

FIG. 16. Integral curves in the presence of damping ($\eta < \mu$, $\nu = 2$).

experimentally observed that addition of dissipation extends the energy bounds for the trapped motions to levels slightly above those obtained for the conservative case.

For $\eta < \mu$ the integral curves are shown in Fig. 16. The reversed direction of the trajectories (spiralling from A) causes a buildup of the x_2 coordinate and we can in general expect a lower stability margin than that for $\eta > \mu$.

4.0. Conclusion. The analysis in the presence of dissipation has revealed one striking observation. The addition of small dissipation properly distributed between the modes causes some of the high-energy solutions which are trapped in the conservative case to decay asymptotically to the origin. A significant feature of this type of solution is its passage through energy levels which in the absence of dissipation would have caused divergence.

REFERENCES

[1] R. Subramanian and R. E. Kronauer, *"Escape" from a potential well. I*, Quart. Appl. Math. (to appear)

[2] R. E. Kronauer and S. A. Musa, *Exchange of energy between oscillations in weakly nonlinear conservative systems*, J. Appl. Mech. ASME **33**, 451–452 (1966)

[3] A. O. Gilchrist, *The free oscillations of conservative quasilinear systems with two degrees of freedom*, Internat. J. Mech. Sci. **3**, 286–311 (1961)